

Increased output of superradiant light-emitting diodes due to population fluctuations

Igor E. Protsenko* and Alexander V. Uskov
P.N.Lebedev Physical Institute of the RAS, Moscow 119991, Russia

The quantum nonlinear Maxwell-Bloch equations for a single-mode laser with a two-level active medium are solved in the LED regime without adiabatic elimination of the medium polarization, when the population fluctuation spectrum is much narrower than the radiation and polarization spectra. It is shown that population fluctuations significantly increase the output power and collective Rabi splitting of a superradiant LED.

Keywords: Super-radiance, nanolasers, quantum noise

I. INTRODUCTION

There is a great demand, interest and progress in the development, study, and application of miniature lasers such as semiconductor lasers [1–3] and nanolasers [4, 5], in particular, surface-emitting [6], photonic crystal [7], microring [8], nanofiber [9], plasmonic [10, 11] lasers and related devices. Theoretical modeling of miniature lasers requires an extension to laser theory, and this paper contributes to this extension. We briefly outline the features of the small lasers we focus on, our previous results and the new contributions made in this paper.

One important feature is a *cavity superradiance*, which appears at a large medium-field coupling in a small, low quality (bad) cavity [12–14]. Many small lasers are superradiant (SR lasers) [15–20]. In small SR lasers, the relaxation rates of the field, the polarization, and the field-medium coupling rate are often similar, meaning the dynamics of all variables in the laser equations are important and must be included in the theory. Consequently, the theory of small SR lasers differs from the standard theory of semiconductor lasers, in which the active medium polarization is eliminated adiabatically [21]. The general motivation behind our theory is to treat the polarization as a dynamical variable. Polarization dynamics in SR lasers reveal new phenomena such as collective Rabi splitting (CRS) [22].

Another important feature of small SR lasers is a their quantum radiation. When there are only a few photons in a small cavity, quantum analysis of lasing is required. The theory of a small SR laser must therefore solve quantum nonlinear equations with at least three dynamical variables: the field, the polarization, and the population of states of the active medium. The problem of solving the quantum nonlinear laser equations is non trivial, and much theoretical work has been done on it in various approximations, for example Refs. [23–29].

Solving quantum nonlinear equations is more challenging than solving classical equations. A detailed comparison of our method with others would require a separate paper. A brief comparison of our method with other approaches is provided below. Consider the mas-

ter equation with the Bogoliubov-Born-Green-Kirkwood-Yvon (BBGKY) hierarchy [29]. In the BBGKY hierarchy, the zero-order approximation neglects field-medium correlations. In our approach, however, such correlations appear already in the zero-order approximation. We believe this is more convenient for calculations. The Heisenberg equations that we use allow for straightforward calculations of observables. They have classical analogues and are more physically transparent than the density matrix equations of Ref.[29]. We are working in the frequency domain, so we do not need to integrate in the time domain, which simplifies the calculations. However, in contrast with Ref.[29], we cannot describe non-stationary processes.

Unlike the quantum rate equation (QRE) theory of [28] and related papers, we do not need the adiabatic elimination of polarization. However, the QRE is very convenient for numerical simulations, whereas a numerical method based on our approach has yet to be developed.

Our theory is similar to the cluster expansion method (the quantum analog of the cumulant-neglect closure [30, 31]). In fact, we perform the cluster expansion in the frequency domain. This allows us to describe phenomena, such as CRS, in field spectra. Unlike our approach, the method of Refs. [15, 25] calculates mean values and correlations, not spectra.

In our papers [22, 32–36] and the present paper, we use Heisenberg equations for SR laser (the quantum Maxwell-Bloch equations with Langevin forces). We make the Fourier expansion of the operators, which has been used in many papers and books, e.g. Refs.[37–39]. The first paper of our approach is Ref.[32], where a thresholdless laser is described neglecting population fluctuations (PF): it is a zero-order approximation to PF. The zero-order approximation allows one to predict collective Rabi splitting, [22]. Following on from Ref. [32], our aim is to take the effect of PFs into account in SR laser theory. The PF produces fluctuations in the number of dipoles and in the polarization, and therefore contributes to the radiation.

In Ref. [33], within the framework of traditional linear perturbation approach, we analyze the effect of PF above the SR laser threshold and predict sideband peaks, caused by PF, in the laser field spectrum. In Ref. [34] we take into account a weak PF effect below laser threshold, in the LED regime, by considering PF as a perturbation.

* procenkoie@lebedev.ru

In Ref. [35] we show that zero-order approximation laser equations are equivalent to the set of equations for normal and inverted harmonic oscillators. Using results of Ref. [35] we show that PF leads to the superthermal photon statistics of a quantum SR LED, as $n \rightarrow 0$ [36].

The present work builds on the research of Refs. [34, 36] on the PF effect in LEDs. The PF effect on LED power is not enough suggested, possibly due to the absence of a suitable theoretical model. Here, we extend the work of Refs. [34, 36] because the perturbative approach of Refs. [34] describes only a weak PF effect. In Ref. [36], however, we observe a significant increase in SR LED power due to PF when n , the number of photons in the LED, is small ($n \rightarrow 0$). This naturally raises the question: is a significant increase in SR LED power due to PF possible for not small n ? This paper is motivated by the desire to answer this important question. Here, we will investigate whether a significant increase in SR LED power by PF is possible when n is not small. In such a case, PF is not a perturbation and the approach of Ref. [34] cannot be used. This motivates us to develop a non-perturbative procedure for solving the nonlinear LED equations. This procedure will be useful for modeling various quantum optical devices. Another motivation was practical: increasing the SR LED power by PF is important for developing efficient miniature light sources. This paper also aims to investigate the effect of PF on collective Rabi splitting in SR LEDs. CRS was considered in Ref. [22] without PF. Here, we will demonstrate that PF increases CRS.

This paper presents three findings. First, we develop a non-perturbative procedure for solving nonlinear quantum Maxwell-Bloch equations with Langevin forces for lasers and quantum optical devices when the population fluctuation spectrum is much narrower than the laser field spectrum. We demonstrate that PFs are a significant source of radiation in the SR LED, increasing its output power by up to 2.5 times. This is the second result. Third, we demonstrate that PF increases the collective Rabi splitting in the LED spectrum.

Section II describes the LED model. The procedure for solving the equations of Sec. II is described in Sec. III, using results from Refs. [34, 36]. Here we take into account the dependence of PF on the cavity photon number n , which was neglected in Ref. [36] as $n \rightarrow 0$ and considered as a perturbation in Ref. [34]. The effect of the PF on the output power and the field spectra of the LED will be demonstrated in Sec. IV. There we compare the effect of PF on non-SR and SR LEDs, formulate conditions for the maximum increase in LED output power and CRS due to PF, and discuss the results. The paper ends with a conclusion.

II. LED MODEL

We consider a stationary regime of the single-mode LED, shown in Fig. 1, with the active medium of N_0

two-level emitters.

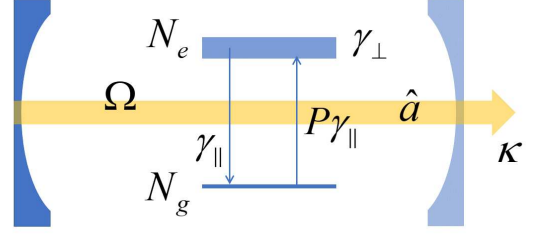


FIG. 1. The scheme of two-level LED model. The field with Bose operator \hat{a} interacts with N_0 two-level atoms (quantum dots) with mean the upper (lower) level populations N_e (N_g), the transition width γ_\perp and the medium-field coupling constant Ω . The upper state decay rate is γ_\parallel and the pump rate is $P\gamma_\parallel$. The cavity field decay rate is κ .

The cavity mode and the transitions of the emitters are in resonance. The LED is described by the Heisenberg-Langevin equations, derived in Ref. [34]

$$\dot{\hat{a}} = -\kappa\hat{a} + \Omega\hat{v} + \sqrt{2\kappa}\hat{a}_{in} \quad (1a)$$

$$\dot{\hat{v}} = -(\gamma_\perp/2)\hat{v} + \Omega f (\hat{a}N + 2\hat{a}\delta\hat{N}_e) + \hat{F}_v \quad (1b)$$

$$\delta\dot{\hat{N}}_e = -\Omega\delta\hat{\Sigma} - \gamma_\parallel(P+1)\delta\hat{N}_e + \hat{F}_{N_e}. \quad (1c)$$

Here $\hat{a}e^{-i\omega_0 t}$ is the cavity field operator with the field amplitude Bose operator \hat{a} and the optical carrier frequency ω_0 ; \hat{v} is the active medium polarization amplitude operator $\hat{v} = \sum_{i=1}^{N_0} f_i \hat{\sigma}_i$; $\hat{\sigma}_i$ is the lowering operator of i -th emitter (see Eqs.(2) of Ref. [34]), f_i describes the difference in the field coupling rates for different emitters; $\delta\hat{N}_e$ is the medium upper state population fluctuation operator; $\delta\hat{\Sigma} = \hat{\Sigma} - \Sigma$ describes fluctuations of the operator $\hat{\Sigma} = \hat{a}^+\hat{v} + \hat{v}^+\hat{a}$ of the dipole interaction between the LED field and the active medium, the mean value of $\hat{\Sigma}$ is Σ ; \hat{a}_{in} is the input vacuum field operator; $\sqrt{2\kappa}\hat{a}_{in}$, \hat{F}_v and \hat{F}_{N_e} are Langevin force operators; κ , $\gamma_\perp/2$ and γ_\parallel are the cavity field, polarization, and upper-state population relaxation rates, respectively; Ω is the Rabi frequency of the field-medium coupling; P is the normalized excitation rate (the pump) of the active medium, the factor $f = N_0^{-1} \sum_{i=1}^{N_0} f_i^2 \approx 1/2$ is due to the averaging over the cavity field and emitter coupling rates, $N = N_e - N_g$ is the mean population inversion, N_g , (N_e) are the mean lower (upper) state populations of the emitters, $N_e + N_g = N_0$. We assume $N_0 \gg 1$.

$N_{e,g}$ can be found from the energy conservation law, which follows from the stationary LED equations for the mean values [22, 32, 34]

$$2\kappa n = \gamma_\parallel(PN_g - N_e), \quad (2)$$

where $n = \langle \hat{a}^+\hat{a} \rangle$ is the mean number of photons in the LED cavity, $n = (2\pi)^{-1} \int_{-\infty}^{\infty} n(\omega) d\omega$, $n(\omega)$ is the cavity

field spectrum,

$$\langle \hat{a}^+(-\omega') \hat{a}(\omega) \rangle = n(\omega) \delta(\omega + \omega'), \quad (3)$$

$\hat{a}(\omega)$ is the Fourier-component of $\hat{a}(t)$:

$$\hat{a}(t) = (2\pi)^{-1/2} \int_{-\infty}^{\infty} \hat{a}(\omega) e^{-i\omega t} d\omega. \quad (4)$$

From Eqs. (1), we find $\hat{a}(\omega)$ as a function of N_e ; calculate $n(\omega)$ and $n(N_e)$ using the correlation properties of the Langevin force operators in Eqs. (1), and find N_e by solving Eq. (2). The same procedure for the calculation of N_e has been performed in Refs. [22, 32] without considering population fluctuations.

To start with, we look again at the estimates that were used before to solve Eqs. (1) in our method, and clarify why a fresh approach is required. Our aim is to describe the effect of PF $\delta\hat{N}_e$ on LEDs. In Eq. (1b), we observe that the nonlinear term, $\sim \hat{a}\delta\hat{N}_e$, contributes to polarization and, consequently, to LED radiation. In the lasing regime, when the radiation line is narrow, \hat{a} can be approximated by a constant, $\hat{a} \approx A$, so $\hat{a}\delta\hat{N}_e \approx A\delta\hat{N}_e$. Then, Eqs. (1) become linear in the operators and can be solved using the standard perturbation procedure, as described in Ref. [33]. However, in the present paper, we do not consider the lasing regime, the radiation line is not narrow; thus, the approximation $\hat{a} \approx A$ cannot be used.

In Refs. [22, 32] we use a zero-order approximation, which neglects $\delta\hat{N}_e$. Then, we solve the linearized equations (1a) (1b) and investigate thresholdless lasing in Ref. [32] and collective Rabi splitting for an SR LED in Ref. [22]. The non linearity $\hat{a}\delta\hat{N}_e$ complicates the calculations in the LED regime, where the usual linearization, as in Ref. [33], is invalid. We then apply the first-order perturbation approach in Ref. [34], replacing \hat{a} in $\hat{a}\delta\hat{N}_e$ with the zero-order approximation result from Refs. [22, 32] and neglecting $\delta\hat{S}$ in Eq. (1c) for $\delta\hat{N}_e$.

The perturbation approach requires that the first-order contribution to be smaller than the zero-order contribution. However, this is not always the case for small SR LEDs, as demonstrated in Ref. [36]. In Ref. [36], we found that population fluctuations significantly increase SR LED power in the strongly quantum regime, when $n \rightarrow 0$. From a practical standpoint, it is interesting to analyze whether a strong increase in LED power is possible when n is not small. In order to perform such an analysis we introduce a *non perturbative* approach, presented in the next section, which takes into account the nonlinear term in Eq. (1b) in the LED regime. We assume that the LED radiation spectrum is broad, the spectral width of the radiation is of the order of $\max\{\kappa, \gamma_{\perp}\}$ and $\kappa, \gamma_{\perp} \gg \gamma_{\parallel} P$ which occurs at typical parameters in the LED regime.

Using the solution of Eqs. (1), we show that PF significantly increase the LED output power not only for

$n \rightarrow 0$, but also when n is not small; PF maintain, and even enhance the collective Rabi splitting [22] in the LED spectra.

III. CALCULATION PROCEDURE

Equations (1) lead to equations for the operators $\hat{a}(\omega)$ and $\hat{v}(\omega)$ of the Fourier components of $\hat{a}(t)$ and $\hat{v}(t)$

$$(\kappa - i\omega)\hat{a}(\omega) = \Omega\hat{v}(\omega) + \sqrt{2\kappa}\hat{a}_{in}(\omega) \quad (5a)$$

$$(\gamma_{\perp}/2 - i\omega)\hat{v}(\omega) = \Omega f \left[\hat{a}(\omega)N + 2(\hat{a}\delta\hat{N}_e)_{\omega} \right] + \hat{F}_v(\omega) \quad (5b)$$

where $(\hat{a}\delta\hat{N}_e)_{\omega}$ is the Fourier component of $\hat{a}\delta\hat{N}_e$. From Eqs. (5a) and (5c) we find

$$\hat{a}(\omega) = \frac{2\Omega^2 f (\hat{a}\delta\hat{N}_e)_{\omega} + \Omega\hat{F}_v(\omega) + (\gamma_{\perp}/2 - i\omega) \sqrt{2\kappa}\hat{a}_{in}(\omega)}{s(\omega)}, \quad (6)$$

where $s(\omega) = (\kappa - i\omega)(\gamma_{\perp}/2 - i\omega) - \kappa\gamma_{\perp}N/2N_{th}$ and $N_{th} = \kappa\gamma_{\perp}/2\Omega^2 f$ is the threshold population inversion found in the semiclassical laser theory [40]. We substitute $\hat{a}(\omega)$ from Eq. (6) into Eq. (3) and calculate the field spectrum

$$n(\omega) = \left[(2\Omega^2 f)^2 S_{aN_e}(\omega) + \gamma_{\perp} f \Omega^2 N_e \right] / |s(\omega)|^2, \quad (7)$$

where $S_{aN_e}(\omega)$ is a convolution

$$S_{aN_e}(\omega) = \frac{1}{2\pi} \int_{-\infty}^{\infty} [n(\omega - \omega') + c(\omega - \omega')/2] \delta^2 N_e(\omega') d\omega', \quad (8)$$

$$c(\omega) = [2\kappa\omega^2 + (\kappa\gamma_{\perp}^2/2)(1 - N/N_{th})] / |s(\omega)|^2 \quad (9)$$

and $\delta^2 N_e(\omega)$ is the power spectrum of PF. For the derivation of Eqs. (7), (8) we use the power spectrum $2D_{v+v}(\omega)$ of the \hat{F}_v Langevin force, $\langle \hat{F}_{v+}(\omega) \hat{F}_v(\omega') \rangle = 2D_{v+v}(\omega) \delta(\omega + \omega')$, found in Refs. [34, 36]

$$2D_{v+v}(\omega) = f\gamma_{\perp}N_e + 2f^2\Omega^2 (c * \delta^2 N_e)_{\omega}, \quad (10)$$

where $(c * \delta^2 N_e)_{\omega}$ is a convolution of $c(\omega)$ and $\delta^2 N_e(\omega)$. In Eq. (5a), \hat{a}_{in} is the vacuum field operator, $\langle \hat{a}_{in}^+(\omega) \hat{a}_{in}(\omega') \rangle = 0$, so $\sqrt{2\kappa}\hat{a}_{in}(\omega)$ does not contribute to $n(\omega)$. In deriving (7), we neglect the correlations between the polarization and population fluctuations, which is an acceptable when N_0 is large. In fact, some of the two photons are most likely emitted by two different emitters with uncorrelated population and polarization fluctuations, as discussed in more detail in Ref. [35].

Let us now discuss the power spectrum (10) of the polarization fluctuations, which describes the sources of

the radiation. The first term on the right-hand side of Eq. (10) comes from the zero-order approximation [22, 32]. It describes the polarization fluctuations of excited emitters. The second term in Eq. (10) appears to satisfy $[\hat{a}, \hat{a}^+] = 1$ when PF is taken into account [34, 36]. The second term is physically equivalent to the PF contribution to spontaneous emission in the LED cavity mode. Meanwhile, the nonlinear term $\hat{a}\delta\hat{N}_e$ in Eq. (1b) describes the PF contribution to stimulated emission.

So, when the number n of photons in the LED approaches zero and the stimulated emission is negligible, the PF effect is mainly described by the second term in Eq. (10), while the nonlinear term $\hat{a}\delta\hat{N}_e$ in Eq. (1b) is neglected [36]. According to the derivation in Refs. [34, 36], the second term in Eq. (10) is not a perturbation. It may exceed the first term, when γ_\perp is small and Ω is large, as in SR LEDs. See examples in Ref. [36], when the second term in Eq. (10) is larger than the first term. The significant contribution of PF at $n \rightarrow 0$ found in Ref. [36] prompted the present study of the PF effect, when n is not small.

We assume that the width of the population fluctuation spectrum $\delta^2 N_e(\omega)$ is much smaller than the widths of the $n(\omega)$ and $c(\omega)$ spectra. In the LED regime, this is true if $\gamma_\parallel \ll \kappa, \gamma_\perp$, which is usually satisfied for semiconductor lasers with fast polarization dephasing and a low quality cavities. Thus, in Eq. (8) we approximate

$$S_{aN_e}(\omega) \approx [n(\omega) + c(\omega)/2]\delta^2 N_e, \quad (11)$$

where $\delta^2 N_e = (2\pi)^{-1} \int_{-\infty}^{\infty} \delta^2 N_e(\omega) d\omega$ is the PF dispersion. Substituting $S_{aN_e}(\omega)$ from Eq. (11) into Eq. (7) we find explicitly the field spectrum in the LED cavity

$$n(\omega) = f\Omega^2 \frac{2\Omega^2 f c(\omega) \delta^2 N_e + \gamma_\perp N_e}{|s(\omega)|^2 - 4\Omega^4 f^2 \delta^2 N_e}, \quad (12)$$

The main difference between the result (12) and the other results [34, 36] is the *nonlinear* dependence of $n(\omega)$ on $\delta^2 N_e$ in (12). The result of Ref. [36] follows from (12) by neglecting the term $\sim \delta^2 N_e$ in the denominator of (12). The result of Ref. [34] can be obtained from (12) using a Taylor expansion of (12) in $\delta^2 N_e$ up to the first-order terms. Thus the results of Refs. [34, 36] are *linear* in $\delta^2 N_e$. The nonlinearity of (12) in $\delta^2 N_e$ may lead to new resonances at high pump power ($P > 1$), when $\delta^2 N_e$ significantly depends on n . We will leave the study of Eq. (12) with a strong pump for the future. Here we will demonstrate that the nonlinearity of Eq. (12) significantly amplifies the impact of PF on the field spectra of SR LEDs when P is about 1.

The population fluctuation dispersion $\delta^2 N_e$ is unknown in Eq. (12). We find $\delta^2 N_e$ using the procedure described in Refs. [34, 35]. There we derive equations for binary operators, such as $\hat{n} = \hat{a}^+ \hat{a}$ and $\hat{\Sigma}$, linearize them respectively to fluctuations and solve them. The procedure of Refs. [34, 35] is valid, if a part $(\delta^2 N_e)_f$ of

$\delta^2 N_e$ caused by the cavity field is small $(\delta^2 N_e)_f^{1/2} \ll N_e$, which is satisfied in this paper.

In Refs. [34, 35], the simplified expression for $\delta^2 N_e$ was used as the mean number of cavity photons $n \rightarrow 0$ and $\delta^2 N_e$ does not depend on n . In contrast to Refs. [34, 35], here n is not small, so that we take into account the dependence of $\delta^2 N_e$ on n .

The result for $\delta^2 N_e$ is a function of N_e , which is an unknown parameter. To find N_e , we insert $\delta^2 N_e(N_e)$ into Eq. (12), calculate the mean photon number $n(N_e) = (2\pi)^{-1} \int_{-\infty}^{\infty} n(\omega) d\omega$, and insert $n(N_e)$ into the law of energy conservation (2). We then find N_e by solving Eq. (2). Substituting N_e into the expression (12) we find the field spectrum $n(\omega)$; integrating $n(\omega)$ over the frequency, we find the mean photon number n .

IV. POPULATION FLUCTUATION EFFECT ON THE LED POWER AND SPECTRA

A. LED parameters

In the examples, we use parameter values close to those typical for semiconductor microlasers and LEDs with quantum dot active media and photonic crystal cavities. The wavelength of the cavity field in vacuum is $\lambda_0 = 1.55 \mu\text{m}$; the linear refractive index of the medium is $n_r = 3.3$. We take the cavity mode volume $V_c = n_c V_{\min}$, where $V_{\min} = (\lambda_0/2n_r)^3$ is the minimum volume of the resonant optical cavity and $n_c \geq 1$ is the normalized cavity volume expressed in V_{\min} units. We have chosen n_c in the region between 2 and 100. The dipole momentum of the two-level emitter (quantum dot) optical transition is $d = 10^{-28} \text{ Cm}$. The Rabi frequency $\Omega = \frac{d}{n_r} \sqrt{\frac{\omega_0}{\varepsilon_0 \hbar V_c}}$, Ω is in the region from $3 \cdot 10^{10}$ to $22 \cdot 10^{10} \text{ rad/s}$ depending on V_c . We consider two values of the polarization decay rate. The first value is $\gamma_\perp = 10^{12} \text{ rad/s}$, which is typical at room temperature [41]. The second value is $\gamma_\perp = 5 \cdot 10^{10} \text{ rad/s}$. This low value of γ_\perp can be achieved by cooling the LED, for example. The decay rate of the cavity field is $\kappa = 2.5 \cdot 10^{10}$ or $\kappa = 5 \cdot 10^{11} \text{ rad/s}$, for cavity quality factors of $2.4 \cdot 10^4$ and $1.2 \cdot 10^3$, respectively. We consider $N_0 = 100$ or $N_0 = 200$ active emitters in the cavity. The decay rate of the upper-state population of the active medium is $\gamma_\parallel = 10^9 \text{ rad/s}$, which is on the order of the spontaneous emission decay rate for the optical dipole transition.

B. LED power and the field spectra

We first consider examples with the LED of a small adiabatic parameter $2\kappa/\gamma_\perp \ll 1$, the superradiance gives a small contribution to the radiation of such a non superradiant (non-SR) LED [22, 34]. In principle, a non-SR LED can be described by the quantum rate equations [21], where the polarization is eliminated adiabatically.

In the first example, we take $\kappa = 2.5 \cdot 10^{10}$ rad/s, $\gamma_{\perp} = 10^{12}$ rad/s, so $2\kappa/\gamma_{\perp} = 0.05 \ll 1$. We consider the values of normalized cavity volume $n_c = 100, 50, 10, 5$, and 2 , so $\Omega = (0.3, 0.43, 0.97, 1.37, 2.17) \cdot 10^{11}$ rad/s, respectively, and $\Omega \ll \gamma_{\perp}$ in all cases, but with $n_c = 2$, when $\Omega = 2.17 \cdot 10^{11} \sim \gamma_{\perp} = 10^{12}$ rad/s. Using the differential gain (the spontaneous emission rate to the cavity mode) $g \equiv 4\Omega^2 f / (2\kappa_0 + \gamma_{\perp})$, we estimate the factor $\beta \equiv g / (g + \gamma_{\parallel}) \sim 1$ is in the region between 0.64 and 0.989 . So the LEDs in all examples have significant spontaneous emission to the cavity mode: the LEDs are thresholdless. We consider $N_0 = 100$ or 200 active emitters in the cavity. We compare results found with the help of the non-perturbative solution Eq. (12) with results obtained in approximations of Refs. [34] and [36].

Figure 2(a) shows the mean output power $p_{out} = 2\kappa n$ (in photons/sec) calculated with (solid lines) and without (dashed lines) PF for the non-SR LED. We see a small contribution of PF to the non-SR LED radiation increasing as the cavity becomes smaller (i.e., for smaller n_c). Fig.2(b) shows the relative LED output power increase $R = p_{out}/p_{out}(\delta N_e = 0)$ due to PF, where $p_{out}[p_{out}(\delta N_e = 0)]$ are the LED powers found with (without) PF. We see that $R > 1$, so PF increases the LED power in all cases. The relative contribution $R - 1$ of PF to the radiation is small, about a few percent, when the polarization decay rate $\gamma_{\perp} \gg \Omega$, as for the four lowest curves in Fig.2(b). The PF contribution increases with the larger active medium and field coupling (smaller cavity volume and larger Ω), as Ω approaches γ_{\perp} , then $R - 1$ reaches $\sim 14\%$ (see the two highest curves in Fig.2 b). R gradually decreases with the pump rate P . Increasing in the number of emitters N_0 does not significantly change R .

The output power spectra $p_{out}(\omega) = 2\kappa n(\omega)$ of the non-SR LED are shown in Fig. 3 for the same parameters as in Fig. 2. Here the PF slightly increases the CRS, e.g. the CRS maxima in curves grow and move to the right much as the normalized cavity volume n_c decreases and the emitter-field coupling rate Ω increases. The PF effect on the CRS is greater for the larger number of emitters (compare curves with $n_c = 2$ and $N_0 = 100$ and 200).

In Figs. 4, we compare the mean output power $p_{out}(P)$ [Fig. 4(a)] and the output power spectra $p_{out}(\omega)$ for $P = 1$ [Fig. 4(b)]. These are found in various approximations for a non-SR LED with $2\kappa/\gamma_{\perp} = 0.05$, $n_c = 2$ and $N_0 = 200$. Curves marked by "no PF" are obtained without PF. Curves marked "PF sp em" are with the effect of PF on spontaneous emission only. Curves with "PF pert" mark are found in the perturbation approach of [34]. Curves marked by "PF exact" are found by the non-perturbative approach of this paper. As shown Figs 4, for non-SR LEDs, we see that PF has a very small effect on spontaneous emission. The perturbative approach of Ref. [34] overestimates the contribution of PF to stimulated emission in Fig. 4(a), while the non-perturbative approach of this paper predicts the maximum change in

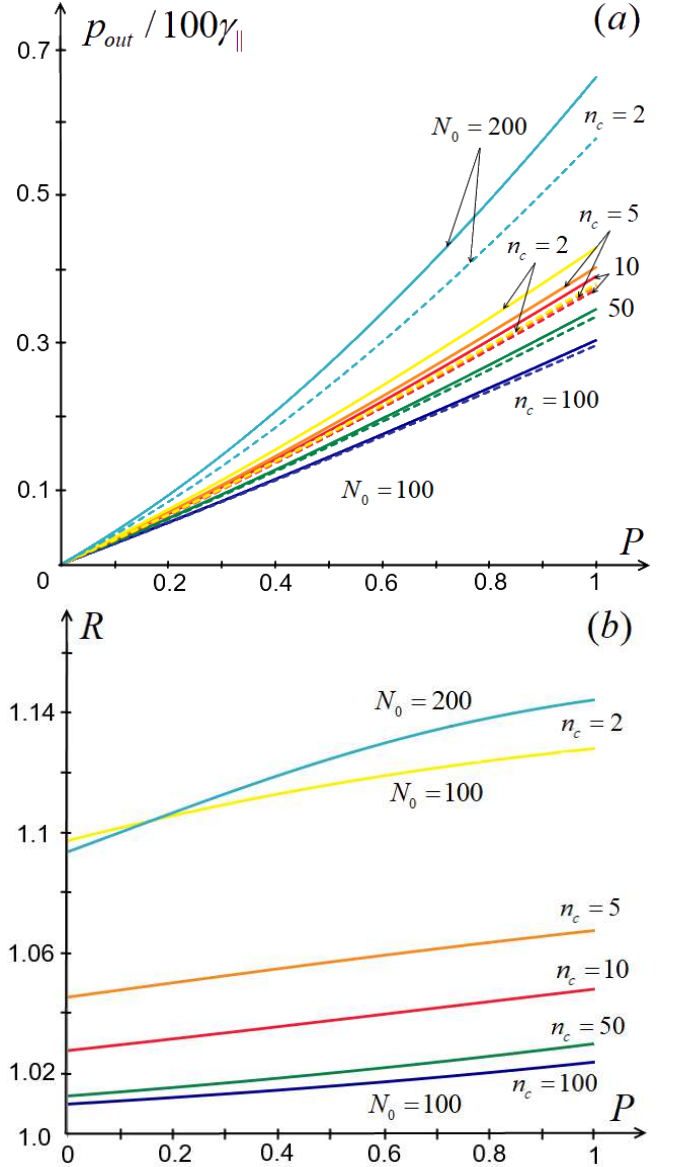


FIG. 2. (a) The mean output power p_{out} (in photons/sec) versus the normalized pump P calculated with (solid curves) and without (dashed curves) PF for the non-SR LED with n_c values shown near curves. The number of emitters $N_0=100$ for all curves but the highest one with $N_0 = 200$. (b) The factor R of the increase the LED output power by PF; notations of curves are the same as in Fig.1a. The PF relative contribution $R - 1$ is small for all curves. R grows with Ω , (i.e. for smaller n_c), remains about the same with the change of N_0 and gradually increases with P , which is explained in the discussion section.

the spectrum $p_{out}(\omega)$ due to PF in Fig. 4(b).

Now we consider the SR LED with a large adiabatic parameter $2\kappa/\gamma_{\perp} > 1$. Note that Eqs. (1) taken without population fluctuations [that is, without $\delta \hat{N}_e$ in Eq. (1b)] have a symmetry: the mean output power and the output power spectrum remain the same in the $2\kappa \leftrightarrow \gamma_{\perp}$

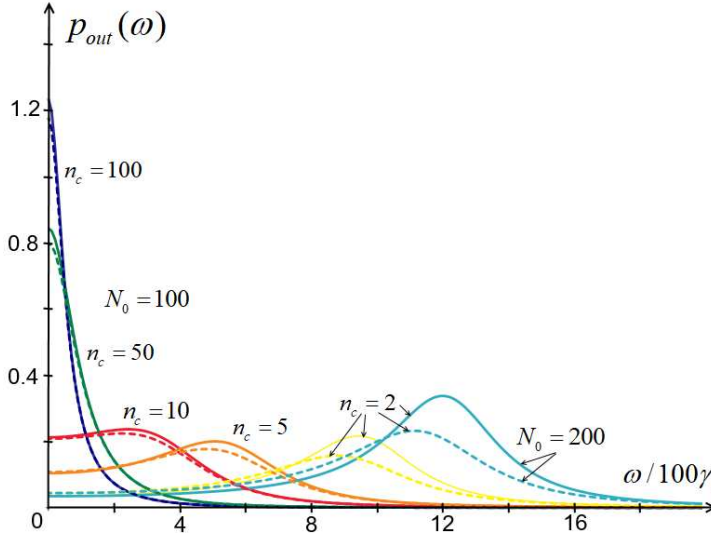


FIG. 3. The output field spectra for non-SR LED for $P = 1$. Parameters for curves are the same as in Fig.2. Solid (dashed) curves are calculated with (without) PF. Values of n_c are shown near curves. Population fluctuations increase and shift the maxima in spectra with CRS to the right i.e. the CRS increases respectively to the case without PF, as much as smaller is the normalized cavity volume n_c . The population fluctuation effect is more visible for larger N_0 (compare curves with $n_c = 2$ and $N_0 = 100, 200$).

exchange. Such a symmetry tells us that the coherence stored in the field in the non-SR LED is transferred to the two-level emitter system in the SR LED. The $2\kappa \leftrightarrow \gamma_\perp$ exchange symmetry is broken when the PFs are taken into account. We take the parameters used in Figs. 2, 3 for non-SR LEDs and make the exchange $2\kappa \leftrightarrow \gamma_\perp$. The adiabatic parameter $2\kappa/\gamma_\perp = 20$ is large after the exchange, so the LED is superradiant.

Fig.5(a) shows the output power $p_{out}(P)$ of the SR LED. Values of parameters are the same as in Fig.2(a), except for the exchange $2\kappa \leftrightarrow \gamma_\perp$. The dashed $p_{out}(P)$ curves calculated without PF are the same as in Fig.2(a). The solid curves are found with PF, and we see that the output power of SR LED is higher than the power of non-SR LED, when PF are taken into account: compare the solid curves in Fig.2(a) and in Fig.5(a).

The relative output power increase R due to PF for SR LED is shown in Fig.5(b) for the same parameters as in Fig.5(a). R grows with Ω/γ_\perp and decreases with P . R for SR LEDs is much higher than for non-SR LEDs, compare the curves with the same n_c in Fig.2(b) and Fig.5(b). The maximum R is $R = 2.5$, see the curve with $n_c = 2$ and $N_0 = 200$.

We observe that R decreases with P in the SR LED [Fig. 2(b)], which differs from the non-SR LED, where R increases with P [Fig. 5(b)]. This is because the PF contributes more to spontaneous emission than to stimulated emission in the SR LED. As P increases, the stimulated

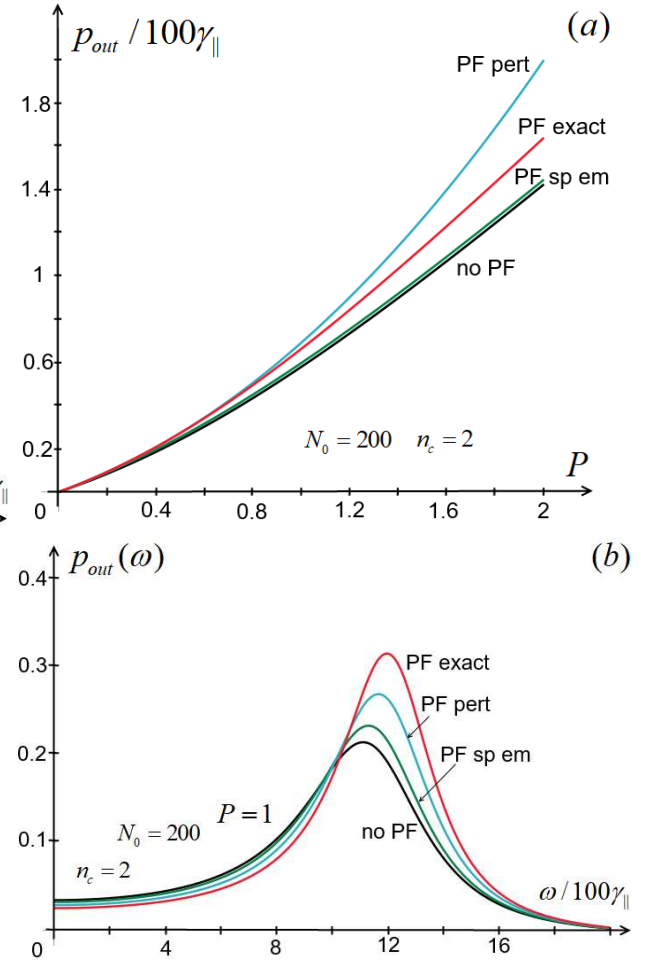


FIG. 4. The mean (a) and the spectrum (b) of the output power of non-SR LED found without PF, with PF effect on the spontaneous emission only, and with the perturbative and non-perturbative PF effect on the LED stimulated emission.

emission dominates the spontaneous emission, reducing the relative PF contribution to the emission of the SR LED and, therefore, reducing R , as shown in Fig. 5(b). In contrast, PF contributes more to stimulated emission than to spontaneous emission in the non-SR LEDs, even for small P . Thus, $R(P)$ increases with P , as shown in Fig 2(b), when stimulated emission increases with P .

The output power spectra $p_{out}(\omega)$ of the SR LED are shown in Fig.6. Here we see a strong effect of PF on $p_{out}(\omega)$, larger than on the spectra of the non-SR LED in Fig.3. The solid curves show that PF significantly increases the CRS - relative to the curves found without PF (dashed curves). The increase and the shift in CRS maxima of SR LED spectra is much greater than for non-SR LED: compare Figs. 3 and 6.

The mean output power p_{out} and the power spectrum $p_{out}(\omega)$ found in Refs. [34, 36] and in this paper for SR LED with $n_c = 2$ $N_0 = 200$ and $2\kappa/\gamma_\perp = 20$ are shown in Figure 7. The notations of the curves are the same

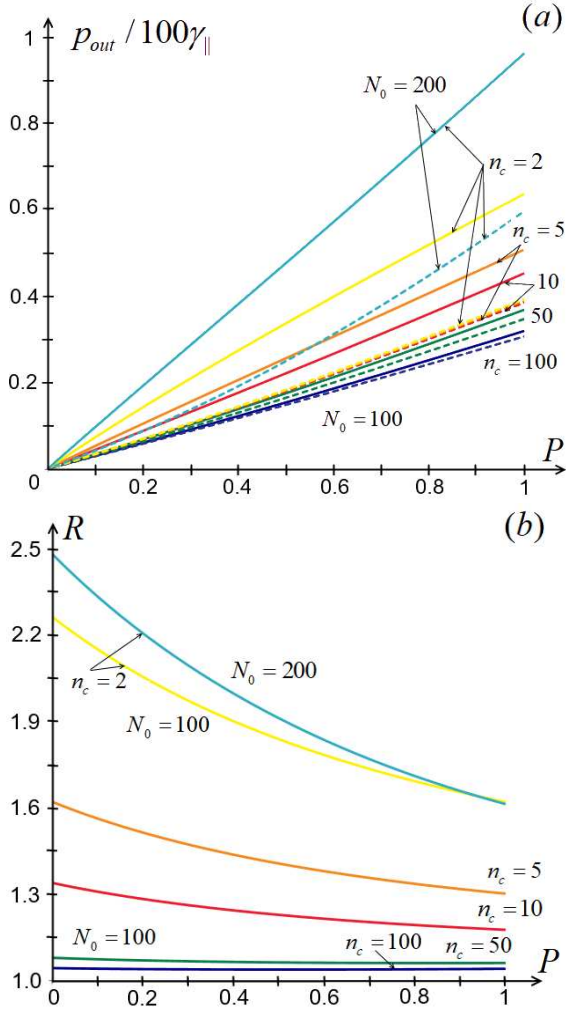


FIG. 5. (a) The output power p_{out} (in photons/sec) of the SR LED as a function of the normalized pump P . Parameter values and the curve numbering are the same as in Fig.2(a), but the value of 2κ is replaced by γ_{\perp} and vice versa. The dashed curves are the same as in Fig.2(a) - due to the symmetry to the $2\kappa \leftrightarrow \gamma_{\perp}$ exchange when Eqs.(1) are without PF. (b) The increase factor R of the LED output power due to PF. R and p_{out} are larger for SR LED than for non-SR LED on Fig.2.

as in Fig. 4. We can clearly see the effect of PF on the SR LED spontaneous emission when P is less than 1. This is different from non-SR LED, where the PF effect on the spontaneous emission is small [compare "no PF" and "PF sp em" curves in Figs. 4(a) and 7(a)]. The field spectrum $p_{out}(\omega)$ is significantly affected by PF, much more than it is in non-SR LED, [see Figs.4(b) and 7(b).] The maximum PF effect on SR spectra is found in the non perturbative approximation of this paper [compare the "no PF" and "PF exact" curves in Fig. 7(b)]. The maximum PF effect on the LED spectra is found in the non-perturbative approach because of a *nonlinear* dependence of $n(\omega)$ on $\delta^2 N_e$ in Eq. (12). This dependence does not appear in the approximations of Refs. [34, 36], which

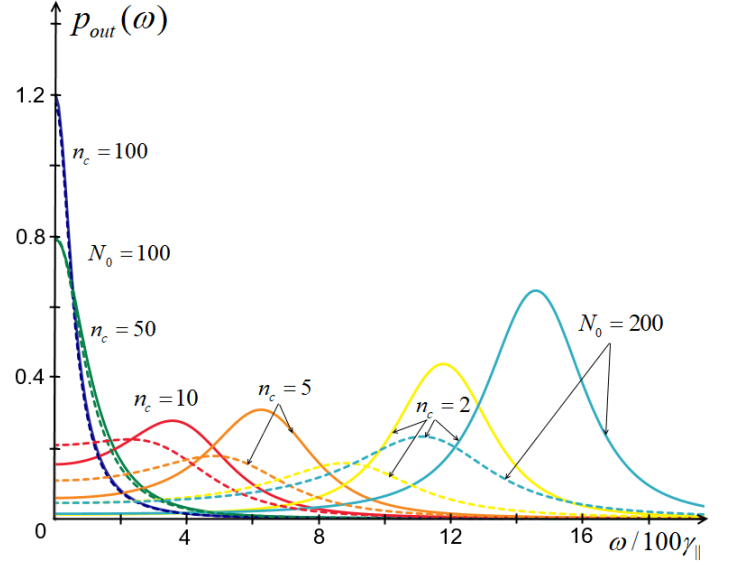


FIG. 6. The output field spectra for SR LED for $P = 1$. Parameters for curves are the same as in Fig.5. Solid (dashed) curves are calculated with (without) PF. Values of n_c are shown near curves. PF increase CRS (shift and enlarge the maxima) much greater than in Fig. 3 for non-SR LED. The PF effect is greater for larger N_0 and smaller n_c (compare curves with $n_c = 2$ and $N_0 = 100, 200$).

are *linear* in $\delta^2 N_e$.

C. Summary and discussion of results

We solve quantum nonlinear Maxwell-Bloch equations (1) below lasing threshold, when the spectrum of the population fluctuation (PF) is narrower than other spectra. The result for the cavity field spectrum $n(\omega)$ is given by Eq. (12). This equation is nonlinear in the PF dispersion $\delta^2 N_e$, which is different to previous approximations in Refs. [34, 36]. Because of the nonlinearity of $n(\omega)$ in $\delta^2 N_e$ PF can strongly affect the LED spectra. Using Eq. (12) we investigate PF as a new source of the LED radiation. We found that PF coupled with the cavity vacuum (or real) field contributes to spontaneous (or stimulated) emission to the cavity mode. We compare the effect of PF on the radiation of the non-SR and SR LEDs for parameters, when LEDs have the same output without PF. We found that PF increased the output and changed the field spectra in SR LED much more than in non-SR LED, see Figs. 2, 5 and Figs 3, 6. We compare the results of different approximations and see that the strongest effect of PF on the field spectra is predicted by the non perturbative approach of this paper.

PF is more important for SR LEDs than non-SR LEDs when it comes to spontaneous emission [see Figs. 4(a) and 7(a)]. This is why the relative contribution R of PF is reduced with the pump P in SR LEDs and increased in

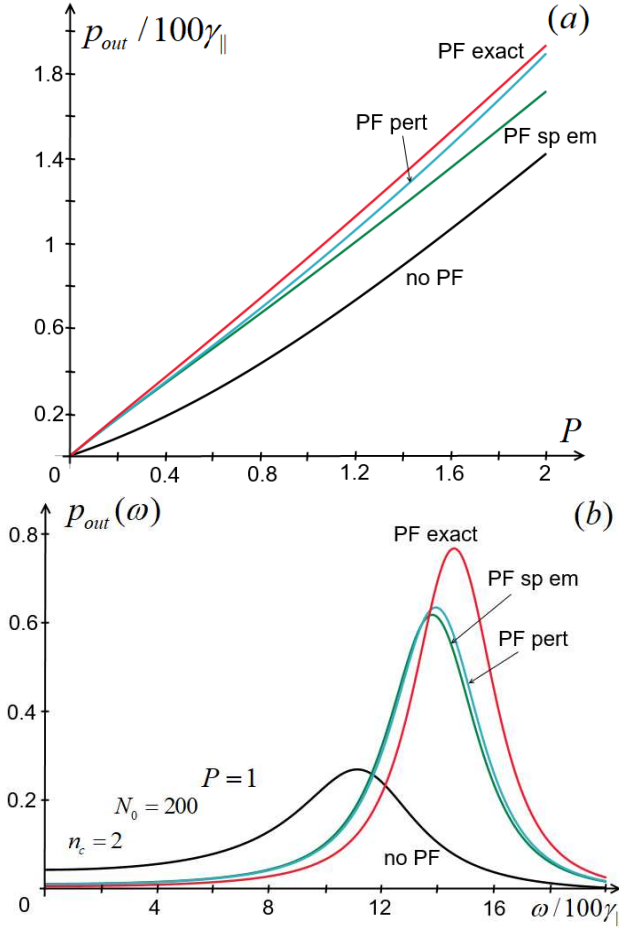


FIG. 7. The mean (a) and the spectrum (b) of the output power of non-SR LED found without PF, with PF effect on the spontaneous emission only, and with the perturbative and non-perturbative account of PF effect on the LED stimulated emission.

non-SR LEDs [see Figs.2(b) and 5(b)]. Therefore, the reason for such $R(P)$ is that stimulated emission overcomes spontaneous emission as P increases.

We see from Eq.(1b) and the polarization Langevin force power spectrum (10) that the contribution of the population fluctuations $\delta\hat{N}_e$ to the polarization is proportional to Ω . The contribution of $\delta\hat{N}_e$ competes with the polarization decay with the rate γ_{\perp} . Therefore, the contribution of PF to the radiation increases with the ratio Ω/γ_{\perp} . This ratio is small for non-SR LEDs, corresponding to the curves in Figs.2: Ω/γ_{\perp} is 0.03, 0.04, 0.1, 0.14 for first four low curves and 0.22 for two top curves. Otherwise, Ω/γ_{\perp} is large for the curves in Figs.5 corresponding to the SR LED, it is 0.61, 0.87, 1.9, 2.7 for the first four and $\Omega/\gamma_{\perp} = 4.3$ for two top curves. Thus, a large medium-field coupling Ω , on the order of γ_{\perp} or larger, and relatively small γ_{\perp} are required for a significant contribution of the PF to the LED radiation. If we consider a non-SR LED with $2\kappa \ll \gamma_{\perp}$, exchanging

$2\kappa \leftrightarrow \gamma_{\perp}$ thus coming to an SR LED after the exchange, we see no difference in the output of such LEDs without considering PF.

Taking PF into account, we see that the PF contributes more to the emission of the SR LED (with a small γ_{\perp}) than to the emission of the non-SR LED (with a large γ_{\perp}). The contribution of PF to spontaneous emission depends on the ratio $\sim \Omega^2/\gamma_{\perp}\gamma_{\parallel}$ of the second (PF) and the first (polarization) terms in the power spectrum (10). This ratio increases with smaller γ_{\perp} . This is why PF's contribution to spontaneous emission is greater for SR LEDs with smaller γ_{\perp} than for non-SR LEDs with larger γ_{\perp} .

The absolute value of PF contribution depends on Ω and the number of emitters N_0 . The value of N_0 does not change much the increase factor R ; see two top curves in Figs.2(b) and 5(b). For values of Ω approaching the maximum (i.e., for the LED cavity size $\sim \lambda/2$), the increase in LED output power due to PF is approximately $R = 2.5$, relative to the radiation power found without PF; see two top curves in Fig.5(b). In Figs. 3, we can see that PF increases the CRS more for SR LED than for non-SR LED. Thus, PF significantly increases the efficiency of SR LEDs and CRS, when $\Omega/\gamma_{\perp} \sim 1$ or greater.

The non-SR LED and SR LED outputs are the same without PF if all LED parameters are the same except for the $2\kappa \leftrightarrow \gamma_{\perp}$ exchange. However, with these parameters, the SR LED output is much larger than the non-SR LED output with PF; compare Figs. 2(a) and 5(a). This is because of the Ω/γ_{\perp} ratio is greater for the SR LED than for the non-SR LED, providing a greater contribution ($\sim \Omega/\gamma_{\perp}$) of PF to the SR LED radiation, as explained above.

Experimental investigations, for example, Refs. [42, 43] of population fluctuations (pump noise [42] or multiplicative noise [43]) have focused on the photon statistics rather than the PF effect on the LED power. Large field intensity fluctuations observed in SR laser experiments [15] can, in principle, be explained by the PF effect [36]. As far as we know, no experiments have been performed to investigate the PF effect on the power of small LEDs. We suggest conducting such an experiment. This can be achieved using photonic crystal LEDs with strong medium-field coupling in a small cavity of the size about the wavelength. For example, one could use two LEDs, as in examples above, with $\kappa = 2.5 \cdot 10^{10}$ rad/s (cavity quality factor $Q = 2.4 \cdot 10^4$) and $5 \cdot 10^{11}$ rad/s ($Q = 1.2 \cdot 10^3$). The high-Q cavity LED operates at room temperature. Therefore, its γ_{\perp} is approximately 10^{12} rad/s and $2\kappa/\gamma_{\perp}$ is much less than 1. It is, therefore, a non-SR LED. The second low-Q cavity LED is cooled to a temperature of about $T = 10 - 15$ K. Assuming $\gamma_{\perp} \sim T$, it has $\gamma_{\perp} \sim 5 \cdot 10^{10}$ rad/s. Thus an exchange of 2κ and γ_{\perp} occurs between the two LEDs, making the low-Q cavity LED superradiant. Our zero-order approximation indicates that outputs of the two LED's should be similar if PF does not affect LEDs. An experimental observation of an increase in the output of

the low-Q cavity LED, relative to the high-Q cavity LED will demonstrate the PF effect in the LED output.

In the future we will study $n(\omega)$, which is nonlinear in $\delta^2 N_e$ according to Eq. (12). We will also study the mean photon number n for a strong pump $P > 1$, when $\delta^2 N_e$ may depend on n . This kind of nonlinearity $n(\delta^2 N_e(n))$ may lead to interesting results, such as resonances, in the dynamics of LEDs and lasers.

Another interesting task for the future is to model the LED regime with a large $P > 1$, when the widths of all spectra are of the same order $\kappa \sim \gamma_\perp \sim \gamma_\parallel$. In this case, the approximation of Eq. (7) by Eq. (12) is invalid. So we have to develop a numerical procedure for finding $n(\omega)$ from the integral equation (12). The population fluctuation power spectrum $\delta^2 N_e(\omega)$ in Eq. (12) can be found using the quantum regression theorem and the Fourier-component operator $\delta \hat{N}_e(\omega)$ determined from Eq. (1c).

V. CONCLUSION

We solve the quantum nonlinear Maxwell-Bloch laser equations in the LED regime, when the population fluctuation power spectrum is much narrower than the field and the polarization spectra. We consider population fluctuations (PF) in the equations using a non perturbative approach and show that PF significantly increase the LED output power: up to 2.5 times under certain conditions. The output field spectra of the SR LEDs are affected by PF. Specifically, PF increases the collective Rabi splitting [22]. The maximum power increase due to PF occurs for the super radiant LEDs when the field-medium coupling (the Rabi frequency) is of the order of or greater than the polarization decay rate. The approach developed in this paper can be used to study of miniature lasers, plasmonic devices [44], and nonlinear quantum optical devices [45].

-
- [1] J. Mørk, Y. Yu, E. Dimopoulos, M. Xiong, M. Salducci, G. Dong, M. Bundgaard-Nielsen, K. Seegert, S. L. Liang, E. Semenova, and K. Yvind, Semiconductor nanolasers, in *2023 Conference on Lasers and Electro-Optics Europe & European Quantum Electronics Conference (CLEO/Europe-EQEC)* (2023) pp. 1–1.
 - [2] D. Saxena, S. Mokkapati, and C. Jagadish, Semiconductor nanolasers, *IEEE Photonics Journal* **4**, 582 (2012).
 - [3] W. Liang, V. S. Ilchenko, D. Eliyahu, A. A. Savchenkov, A. B. Matsko, D. Seidel, and L. Maleki, Ultralow noise miniature external cavity semiconductor laser, *Nature Communications* **6**, 7371 (2015).
 - [4] R.-M. Ma and R. F. Oulton, Applications of nanolasers, *Nature Nanotechnology* **14**, 12 (2019).
 - [5] K.-Y. Jeong, M.-S. Hwang, J. Kim, J.-S. Park, J. M. Lee, and H.-G. Park, Recent progress in nanolaser technology, *Advanced Materials* **32**, 2001996 (2020).
 - [6] C.-Y. Lu, S. L. Chuang, and D. Bimberg, Metal-cavity surface-emitting nanolasers, *IEEE Journal of Quantum Electronics* **49**, 114 (2013).
 - [7] D. Fitsios and F. Raineri, Chapter five - photonic crystal lasers and nanolasers on silicon, in *Silicon Photonics*, Semiconductors and Semimetals, Vol. 99, edited by S. Lourdudoss, R. T. Chen, and C. Jagadish (Elsevier, 2018) pp. 97–137.
 - [8] W. W. Wong, Z. Su, N. Wang, C. Jagadish, and H. H. Tan, Epitaxially grown inp micro-ring lasers, *Nano Letters* **21**, 5681 (2021).
 - [9] S. Li, W.-F. Jiang, Y.-P. Xu, and T. F. George, Invisible cavity of a polymeric nanofiber laser, *The Journal of Physical Chemistry C* **115**, 17582 (2011).
 - [10] M. A. Noginov, G. Zhu, A. M. Belgrave, R. Bakker, V. M. Shalaev, E. E. Narimanov, S. Stout, E. Herz, T. Suteewong, and U. Wiesner, Demonstration of a spaser-based nanolaser, *Nature* **460**, 1110 (2009).
 - [11] M. A. Noginov and J. B. Khurgin, Is metal a friend or foe?, *Nature Materials* **17**, 116 (2018).
 - [12] Y. I. Khanin, *Fundamentals of laser dynamics* (Cambridge International Science Pub, 2005).
 - [13] A. A. Belyanin, V. V. Kocharovskiy, and V. V. Kocharovskiy, Superradiant generation of femtosecond pulses in quantum-well heterostructures, *Quant. Semiclass. Opt.: JEOS Part B* **10**, L13 (1998).
 - [14] V. V. Kocharovskiy, V. V. Zheleznyakov, E. R. Kocharovskaya, and V. V. Kocharovskiy, Superradiance: the principles of generation and implementation in lasers, *Physics-Uspekhi* **60**, 345 (2017).
 - [15] F. Jahnke, C. Gies, M. Aßmann, M. Bayer, H. A. M. Leymann, A. Foerster, J. Wiersig, C. Schneider, M. Kamp, and S. Höfling, Giant photon bunching, superradiant pulse emission and excitation trapping in quantum-dot nanolasers, *Nature Commun.* **7**, 11540 (2016).
 - [16] M. A. Norcia and J. K. Thompson, Cold-strontium laser in the superradiant crossover regime, *Phys. Rev. X* **6**, 011025 (2016).
 - [17] S. A. Schäffer, B. T. R. Christensen, M. R. Henriksen, and J. W. Thomsen, Dynamics of bad-cavity-enhanced interaction with cold Sr atoms for laser stabilization, *Phys. Rev. A* **96**, 013847 (2017).
 - [18] D. Meiser and M. J. Holland, Steady-state superradiance with alkaline-earth-metal atoms, *Phys. Rev. A* **81**, 033847 (2010).
 - [19] K. Debnath, Y. Zhang, and K. Mølmer, Lasing in the superradiant crossover regime, *Phys. Rev. A* **98**, 063837 (2018).
 - [20] J. G. Bohnet, Z. Chen, J. M. Weiner, D. Meiser, M. J. Holland, and J. K. Thompson, A steady-state superradiant laser with less than one intracavity photon, *Nature* **484**, 78 (2012).
 - [21] L. A. Coldren, S. W. Corzine, and M. L. Masanovic, *Diode lasers and photonic integrated circuits* (Wiley, 2nd ed., 2012).
 - [22] E. C. André, I. E. Protsenko, A. V. Uskov, J. Mørk, and M. Wubs, On collective Rabi splitting in nanolasers and nano-LEDs, *Opt. Lett.* **44**, 1415 (2019).
 - [23] E. C. André, J. Mørk, and M. Wubs, Efficient stochastic simulation of rate equations and photon statistics of nanolasers, *Opt. Express* **28**, 32632 (2020).

- [24] M. I. Kolobov, L. Davidovich, E. Giacobino, and C. Fabre, Role of pumping statistics and dynamics of atomic polarization in quantum fluctuations of laser sources, *Phys. Rev. A* **47**, 1431 (1993).
- [25] C. Gies, J. Wiersig, M. Lorke, and F. Jahnke, Semiconductor model for quantum-dot-based microcavity lasers, *Phys. Rev. A* **75**, 013803 (2007).
- [26] N. Gregersen, T. Suhr, M. Lorke, and J. Morek, Quantum-dot nano-cavity lasers with purcell-enhanced stimulated emission, *Applied Physics Letters* **100**, 131107 (2012).
- [27] J. Mørk and G. L. Lippi, Rate equation description of quantum noise in nanolasers with few emitters, *Appl. Phys. Lett.* **112**, 141103 (2018).
- [28] F. Papoff, M. A. Carroll, G. L. Lippi, G.-L. Oppo, and G. D'Alessandro, Quantum correlations, mixed states, and bistability at the onset of lasing, *Phys. Rev. A* **111**, L011501 (2025).
- [29] N. A. Lozing, E. A. Tarasevich, V. K. Roerich, and M. G. Gladush, Fully quantum-kinetic theory of the steady-state cooperative photoluminescence from two near-identical emitters, *Physica E: Low-dimensional Systems and Nanostructures* **164**, 116061 (2024).
- [30] W. Wu and Y. Lin, Cumulant-neglect closure for nonlinear oscillators under random parametric and external excitations, *International Journal of Non-Linear Mechanics* **19**, 349 (1984).
- [31] J.-Q. Sun and C. S. Hsu, Cumulant-Neglect Closure Method for Nonlinear Systems Under Random Excitations, *Journal of Applied Mechanics* **54**, 649 (1987).
- [32] I. Protzenko, P. Domokos, V. Lefèvre-Seguin, J. Hare, J. M. Raimond, and L. Davidovich, Quantum theory of a thresholdless laser, *Phys. Rev. A* **59**, 1667 (1999).
- [33] I. E. Protzenko, A. V. Uskov, E. C. André, J. Mørk, and M. Wubs, Quantum langevin approach for superradiant nanolasers, *New Journal of Physics* **23**, 063010 (2021).
- [34] I. E. Protzenko and A. V. Uskov, Perturbation approach in heisenberg equations for lasers, *Phys. Rev. A* **105**, 053713 (2022).
- [35] I. E. Protzenko and A. V. Uskov, Oscillator laser model, *Annalen der Physik* **535**, 2200298 (2023).
- [36] I. E. Protzenko and A. V. Uskov, Population fluctuation mechanism of the super-thermal photon statistic of quantum leds with collective effects, *Annalen der Physik* **536**, 2400121 (2024).
- [37] G. P. Agrawal and G. R. Gray, Intensity and phase noise in microcavity surface-emitting semiconductor lasers, *Applied Physics Letters* **59**, 399 (1991).
- [38] L. Davidovich, Sub-Poissonian processes in quantum optics, *Rev. Mod. Phys.* **68**, 127 (1996).
- [39] M. S. Scully, M. O. Zubairy, *Quantum Optics* (Cambridge University Press, 1997).
- [40] M. Sargent, M. O. Scully, and W. E. Lamb, *Laser Physics* (London : Addison-Wesley, 1974).
- [41] U. Bockelmann and T. Egeler, Electron relaxation in quantum dots by means of Auger processes, *Phys. Rev. B* **46**, 15574 (1992).
- [42] S. B. Foster and A. E. Tikhomirov, Pump-noise contribution to frequency noise and linewidth of distributed-feedback fiber lasers, *IEEE Journal of Quantum Electronics* **46**, 734 (2010).
- [43] P. Lett, R. Short, and L. Mandel, Photon statistics of a dye laser far below threshold, *Phys. Rev. Lett.* **52**, 341 (1984).
- [44] I. E. Protzenko, A. V. Uskov, and N. V. Nikonorov, Spontaneous emission, collective phenomena and the efficiency of plasmon-stimulated photoexcitation, *Photonics and Nanostructures - Fundamentals and Applications* **61**, 101297 (2024).
- [45] I. E. Protzenko and A. V. Uskov, Single-photon optical bistability in a small nonlinear cavity, *Phys. Rev. A* **108**, 023724 (2023).